PROCEEDINGS OF THE ROYAL SOCIETY A MATHEMATICAL, PHYSICAL & ENGINEERING SCIENCES

V. Studies of Cosmic Ray Neutrino Interactions in the Kolar Gold Field Experiment

M. G. K. Menon, S. Naranan, V. S. Narasimham, K. Hinotani, N. Ito, S. Miyake,
R. Craig, D. R. Creed, J. L. Osborne and A. W. Wolfendale

Proc. R. Soc. Lond. A 1967 **301**, 137-157
doi: 10.1098/rspa.1967.0197

Proc. Roy. Soc. A. **301**, 137–157 (1967)
Printed in Great Britain

V. Studies of cosmic ray neutrino interactions in the Kolar Gold Field experiment

By M. G. K. Menon, S. Naranan and V. S. Narasimham
Tata Institute of Fundamental Research, Bombay, India

K. Hinotani, N. Ito and S. Miyake
Osaka City University, Osaka, Japan

and R. Craig, D. R. Creed, J. L. Osborne and A. W. Wolfendale
University of Durham, Durham, U.K.

[Plates 22 and 23]

Results are presented of an experiment to study the penetrating particles in the cosmic radiation deep underground, at a depth of 7500 m.w.e. (standard rock). The events recorded are attributable, in the main, to muons produced either in the atmosphere or by the interactions of neutrinos in the surrounding rock.

The muons have been studied in some detail and it appears that the mean energy of the neutrino induced muons (probably less than about 30 GeV) is low compared with that of the muons of atmospheric origin.

The significance of the celestial coordinates of the muons and the measured rate of neutrino-induced muons is discussed and the future experimental programme is indicated.

1. Introduction

It had long been realized that there should be a flux of neutrinos in the cosmic radiation but it was only in 1965 that direct evidence for their existence was obtained. This evidence came from the observation of particles incident on detectors placed deep underground which were most easily interpreted as the secondaries of neutrino interactions (Achar *et al.* 1965*a*; Reines *et al.* 1965). The purpose of the present paper is to summarize the present status of the Kolar Gold Field experiment.

Before continuing with a detailed description of the apparatus and the latest results it is useful to review briefly the sources of the neutrinos which should be present at ground level and below. Figure 1 shows the sequence of events leading to the production of both electron and muon neutrinos. In the absence of surprises, in the form of intense fluxes of neutrinos from unusual celestial objects, the majority of electron neutrinos, which have energies in the MeV region, come from the sun and the bulk of the muon neutrinos (and $\bar{\nu}_{\mu}$) arise from the decays of the secondary cosmic rays in the atmosphere.

The very small cross-section for neutrino interactions dictates that experimental studies be carried out deep underground where background effects are low. Since high energy muon neutrinos give penetrating muon secondaries, such particles are somewhat easier to detect and the experimental arrangement is designed with the object of recording these muons. The detection of muon neutrinos is, in fact, possible only because the great penetration of the secondary muons yields a large target thickness in the surrounding rock which offsets in part the rapidly falling neutrino energy spectrum.

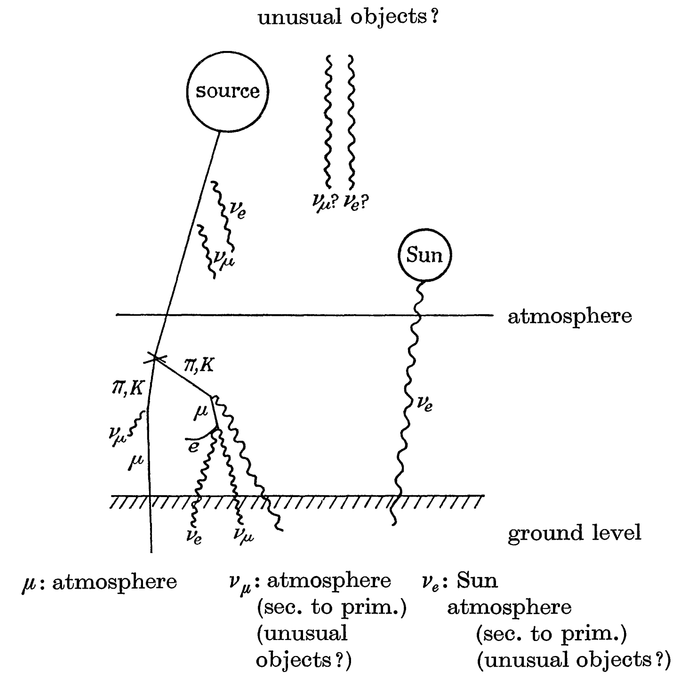

FIGURE 1. Sources of cosmic ray neutrinos and muons.

From a knowledge of the details of the propagation of cosmic rays in the atmosphere the energy spectrum of the neutrinos (ν_μ, $\bar{\nu}_\mu$, ν_e and $\bar{\nu}_e$) can be calculated with reasonable accuracy. Thus, if the frequency of the neutrino-induced secondary muons is determined experimentally the cross-section for neutrino interaction can be studied. More specifically, the predictions of particular neutrino interaction models can be checked; the interest in this lying in the fact that much of the contribution to the measured frequency comes from neutrinos of energy above that currently available from accelerating machines. Another aspect of great theoretical interest concerns the existence, or otherwise, of the intermediate boson. Such a particle has not been detected in accelerator experiments and if it exists its mass is consequently above 1·8 GeV; if it has a mass below about 4 GeV it should be detectable during the course of the present experiment.

The possibility of extra-terrestrial sources has already been mentioned. Results of the analysis from the present work on the celestial coordinates of the arrival directions of the neutrinos will be given.

There have been three successive reports of the results of the present experiment: by Achar *et al.* (1965*a–c*). The present data, which are twice as numerous as those previously reported, include observations with new apparatus and the improvement in estimate of the cross-section will be examined and the nature of the interactions will be discussed.

2. The experimental arrangement

The detectors are located in the Kolar Gold Mines in South India at a depth of 7600 ft. (equivalent to 7500 m water equivalent (m.w.e.) in the case of 'standard rock' with $Z^2/A = 5{\cdot}5$). At this depth the intensity of atmospheric muons in the vertical direction is down by a factor of 10^8 compared with ground level. The intensity of these muons falls off with zenith angle θ, at a rate somewhat faster than $\cos^8\theta$; the actual variation has been discussed by Menon *et al.* (1967).

2·1. *Telescopes* 1 *and* 2

Two types of 'telescopes' have been installed. The first type comprises two identical telescopes (1 and 2), each consisting of two vertical walls of plastic scintillators 2 m long and 3 m high separated by 80 cm, as shown in figure 2. Each 'scintillator element', 1 m² in area, is viewed by two adjacent 5 in. diameter photomultipliers; fourfold coincidences are recorded between a pair of photomultipliers on one wall and any pair on the other wall. Between the scintillator

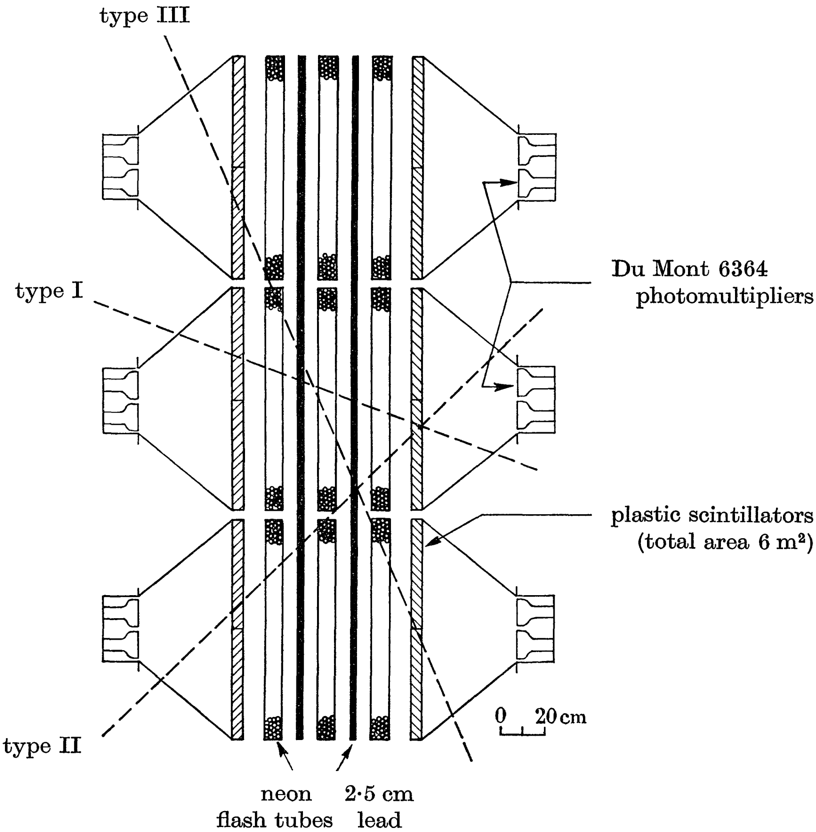

Figure 2. Geometrical arrangement of telescopes 1 and 2.

walls there are three arrays of neon flash tubes and in each array there are four columns of flash tubes. There are two walls of lead absorber, each 2·5 cm in thickness, between the flash tube arrays. When fourfold coincidences occur, the photomultiplier pulses are recorded on oscilloscopes, and after a delay of about 30 μs a high voltage pulse is applied to the electrodes of the neon flash tube arrays. The resulting flashes are photographed by two cameras for each telescope which view the tubes directly.

The effective aperture offered by each of the telescopes is about 0·22 m^2 sr, for atmospheric muons and is about 20 m^2 sr for an isotropically distributed radiation; neutrino-induced muons are expected to correspond approximately to this. The flash tubes, which are of length 200 cm and diameter 1·8 cm, enable the projected zenith angles of single tracks to be measured to an accuracy of about 1°. The determination of azimuthal angle is poor, however, being given only from a knowledge of the pattern of scintillators traversed.

2·2. *Telescopes* 3 *to* 5

In order to improve the accuracy of azimuthal angle and also to increase the potentialities for distinguishing between muons and pions three telescopes of a different type have been installed (telescopes 3, 4 and 5, figure 3). In these tele-

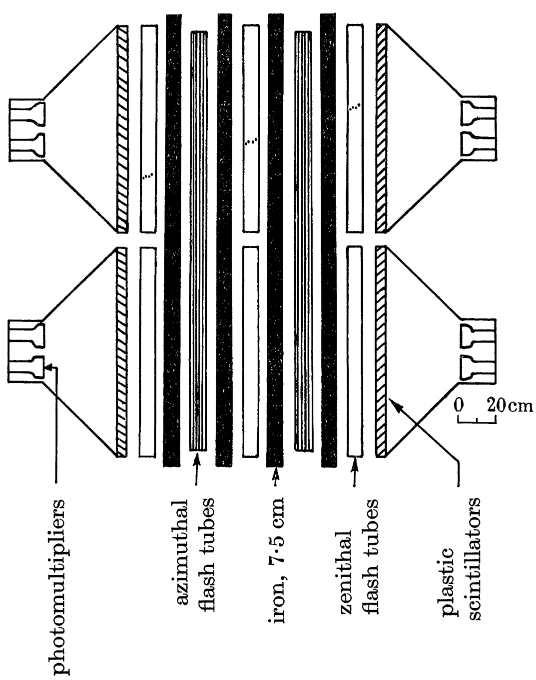

Figure 3. Geometrical arrangement of telescopes 3 to 5.

scopes the triggering elements comprise two walls of plastic scintillators each of area 4 m^2 separated by a horizontal distance of 130 cm. The absorber comprises four columns of iron, each 7·5 cm thick, which are interposed between the flash-tube arrays. There are five arrays of flash tubes arranged in a crossed configuration with three arrays of horizontal tubes and two arrays of vertical tubes. As with telescopes 1 and 2 there are four layers of tubes in each array. All five arrays of tubes are photographed by a single camera through a mirror system. The result of using the crossed arrays is that the spatial zenith angles of single tracks can be measured to an accuracy of about 1°. Owing to the smaller area and larger separation of the scintillators the effective aperture of each of these telescopes is less than those of telescopes 1 and 2, being 7·9 m^2 sr for an isotropically distributed radiation.

2·3. *The disposition of the telescopes*

The five telescopes are operated in the same tunnel, disposed as shown schematically in figure 4. The horizontal tubes lie approximately in the east–west direction.

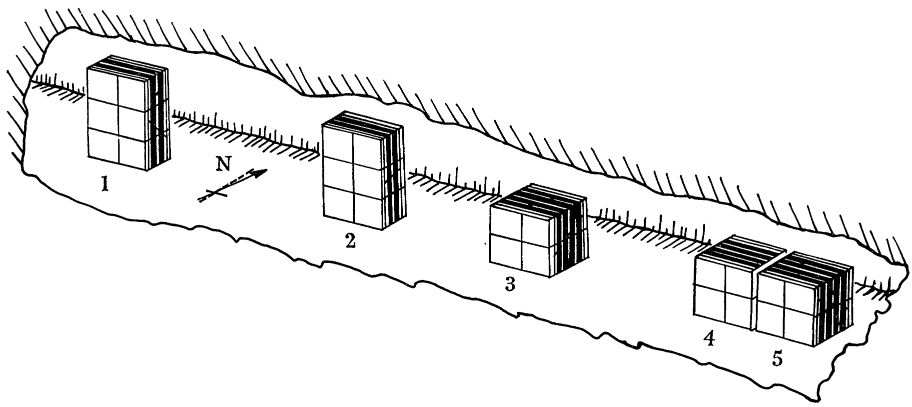

FIGURE 4. Disposition of telescopes in tunnel.

The coincidence arrangements for telescopes 4 and 5 are modified so that oblique particles passing from one side of one telescope to the opposite side of the other also provide triggering pulses, thereby increasing the acceptance somewhat.

3. BASIC DATA

3·1. *Exposure*

The original two telescopes (1 and 2) have been in operation since the beginning of 1965 and up to 1 October 1966 the accumulated exposure corresponded to 13128 m^2 day sr. The new telescopes (3, 4 and 5) were commissioned early in 1966 and by the same date had accumulated a running time of 3787 m^2 day sr. The data are thus based on a total exposure corresponding to 16915 m^2 day sr ($1·46 \times 10^{13}$ cm^2 s sr; all the exposures corresponding to an isotropic radiation).

3·2. *Classes of events recorded*

Thirty-two events have been recorded (see table 1) and their break-down according to type is given in table 2. Those events corresponding to the passage of penetrating particles through the scintillation counters on both sides of the telescopes (i.e. 'in geometry' events) are shown in figure 5 plotted with respect to projected zenith angle for telescopes 1 and 2 and spatial zenith angle for telescopes 3 to 5.

TABLE 1. EVENTS OBTAINED IN THE K.G.F. NEUTRINO EXPERIMENT UP TO 1 OCTOBER 1966

event no.	date and time I.S.T. (h, min)	coincidence	event type	projected zenith angle (deg)	remarks
1	5. iv. 65 20, 04	S_4 N_4 tel. 2	I	> 37	neon flash tubes are not present
2	27. iv. 65 18, 26	S_1 N_1 tel. 1	I	48 ± 1	only two extreme trays of neon flash tubes are present
3	25. v. 65 20, 03	S_6 N_6 tel. 2	I	75 ± 10	only the central tray of neon flash tubes is present
4	3. vii. 65 12, 30	S_1 N_1 tel. 2	I	96·2 ± 0·8 99·2 ± 0·3	double track event
5	13. vii. 65 16, 13	$S_{3,5,6}$ N_4 tel. 2	II	45 ± 1	—
6	18. vii. 65 02, 52	$S_{1,2}$ $N_{3,6}$ tel. 1	out of geom.	8·5 ± 1	—
7	24. vii. 65 11, 47	S_3 N_6 tel. 2	II	37·5 ± 1	—
8	27. vii. 65 03, 24	S_3 N_6 tel. 1	II	29·5 ± 1	—
9	29. vii. 65 19, 07	S_3 N_1 tel. 2	II	32·5 ± 2·5	—
10	1. viii. 65 21, 00	— tel. 1	out of geom.	25 ± 1	oscilloscope data not available
11	2. viii. 65 03, 38	S_4 N_6 tel. 1	II	47 ± 1	—
12	11. viii. 65 17, 37	S_5 N_4 tel. 1	out of geom.	33 ± 1	—
13	12. viii. 65 11, 38	$S_{1,2,6}$ $N_{2,4,6}$ tel. 1 S_{all} $N_{1,2,4,5,6}$ tel. 2	?	?	neon flash tube data: big shower in tel. 2 nothing in tel. 1
14	9. ix. 65 02, 22	$S_{1,3}$ N_5 tel. 2	III	21 ± 1	shower in middle and south sections of n.f.t. of tel. 2
15	10. ix. 65 08, 20	S_3 N_6 tel. 1	II	26·5 ± 1	—
16	13. x. 65 12, 14	S_1 N_3 tel. 1	II	40 ± 1	no flashes in north-wing n.f.t.
17	13. i. 66 20, 30	S_2 N_6 tel. 2	III	?	no n.f.t. information
18	26. i. 66 03, 38	S_5 N_4 tel. 1	II	36 ± 1	knock-on in south-wing n.f.t.
19	27. i. 66 02, 23	no information tel. 1	II	33 ± 1	knock-on in central n.f.t. also penetrating to south-wing n.f.t.
20	5. ii. 66 04, 28	S_4 N_6 tel. 2	II	51·5 ± 1	knock-on in central n.f.t.
21	14. iii. 66 06, 02	S_5 $N_{2,4,6}$ tel. 1	out of geom.	near vertical?	shower—largest number of flashes in north-wing n.f.t.
22	9. v. 66 13, 31	S_1 N_3 tel. 5	II	46·2 ± 0·2	knock-on in south azimuthal n.f.t.
23	9. v. 66 17, 42	no information tel. 2	I	44·6 ± 1	—
24	25. v. 66 00, 01	$S_{1,3,5}$ N_4 tel. 1	out of geom.	—	big shower in south-wing n.f.t.

TABLE 1 (*cont.*)

event no.	date and time I.S.T. (h, min)	coincidence	event type	projected zenith angle (deg)	remarks
25	9. vi. 66 12, 47	S_1 N_3 tel. 2	II	$44{\cdot}1 \pm 1$	knock-on in south-wing n.f.t.
26	16. vi. 66 18, 32	$S_{4,5}$ N_2 tel. 2	III	$19{\cdot}4 \pm 1$	knock-on in north-wing n.f.t.
27	27. vi. 66 16, 06	S_6 N_4 tel. 2	II	$42{\cdot}8 \pm 1$	knock-on in south-wing n.f.t.
28	29. vi. 66 21, 06	S_3 N_3 tel. 3	out of geom.	10 ± 1	—
29	29. vi. 66 22, 15	$S_{1,2,4,5}$ $N_{1,3,4}$ tel. 1	I	47, 97, 155	the three tracks seem to meet at *ca.* 60 cm from the scintillators in the south-wing
30	18. vii. 66 20, 37	S_1 tel. 5 N_1 tel. 4	I	72 ± 1	—
31	6. viii. 66 16. 33	$S_{1,3}$ N_6 tel. 2	III	21 ± 4	—
32	4. ix. 66 05, 54	$S_{1,3}$ $N_{2,3,4,5,6}$ tel. 1	II	26 ± 1	muon accompanied by secondaries and shower produced in lead absorber

The angles of the events in tels. 3 to 5 are spatial zenith angles. I.S.T. denotes Indian Standard Time.

Under the heading 'coincidence' S and N denote south and north and the suffixes correspond to the serial numbers of the scintillators traversed (these are numbered in pairs from the bottom).

TABLE 2. BREAKDOWN OF DETECTED EVENTS

category	tels. 1 and 2	tels. 3 to 5
atmospheric muons + neutrino muons ($\phi < 40°$)	10	—
intermediate ($40° < \phi < 50°$)	7	1
neutrino muons ($\phi > 50°$)	4	1
out of geometry single tracks	3	1
electron showers	3	—
flash tubes off	2	—
(photon showers?)	(1)	(1)
total	29(+1)	3(+1)

Also shown in figure 5 is the distribution in projected angle expected for muons of atmospheric origin, i.e. muons which have penetrated the overlying earth from ground level. This distribution has been calculated from the work of Menon *et al.* (1967) in which an analysis was made of the depth-intensity relation and the angular distribution expected at great depths. (Essentially the same distribution results if it is assumed that all the muons with $\phi < 35°$ are of atmospheric origin.) In deriving this distribution it is assumed that the effect of any unusual interaction of muons which gives rise to significant deflexions in the overlying rock is very small; the broadening of the distribution by Coulomb scattering having been shown to be negligible.

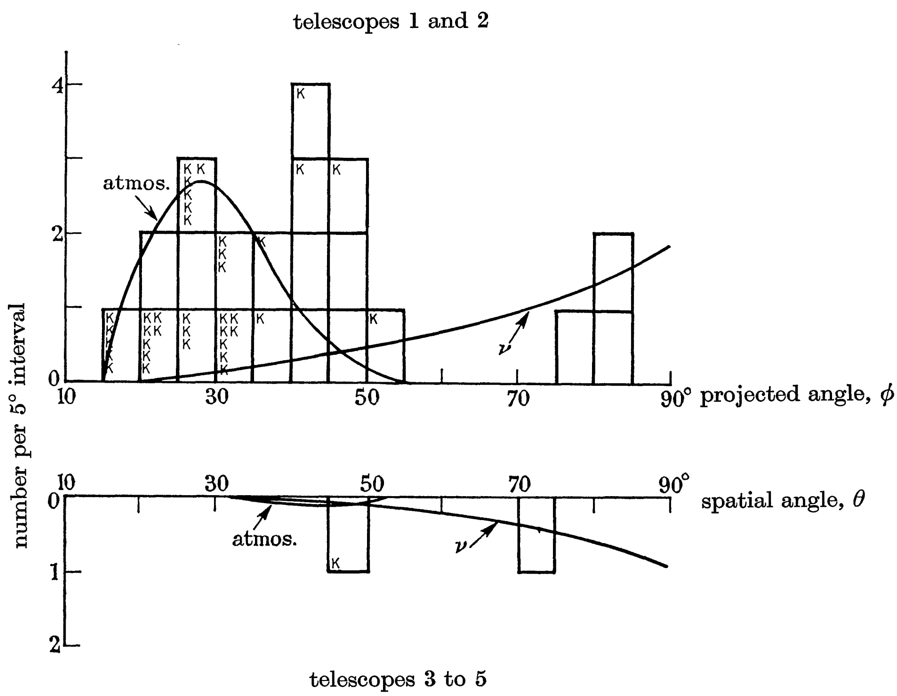

FIGURE 5. Angular distribution of the 'in-geometry' events (K denotes an electron associated with the muon).

The derivation of the exact number of neutrino-induced muons from the data is difficult. At angles above 50° it is clear that all the events are due to neutrinos, but in the region of 40 to 50° where comparable numbers of atmospheric and neutrino-induced muons are expected the division between the two is uncertain. The peak at an angle of *ca.* 45° is hard to understand, but on the assumption that the excess above expectation is as likely to be in the number of neutrino-induced muons as in the atmospheric muons it is concluded that between 8 and 11 of the events are neutrino-induced. Accordingly, the number of in-geometry atmospheric muons is 12 to 15. Further analysis of this intriguing peak, which appears to be associated with low energy muons and may indicate some new process, is continuing.

In addition to the events with penetrating particles traversing the scintillators seven events were detected in which the necessary 'trigger' was provided either by a secondary accompanying a penetrating particle or by an electron shower. One of these showers was particularly big and corresponded to an energy content of at least several hundred GeV.

Finally, two events were seen (not included in the 32) which were probably due to weak photon showers incident on the telescopes.

Of the photographs showing in-geometry events two were notable in showing accompaniment which could not easily be explained in terms of electromagnetic phenomena. These events are attributable to non-elastic neutrino interactions and will be discussed in some detail later.

Photographs of some of the events are shown in figures 14 to 20, plates 22 and 23.

4. Detailed analysis of the data and discussion of the results

4·1. *Nature of the detected particles*

In the absence of any surprises the particles expected to be present underground in significant fluxes are the following:

muons of atmospheric origin and sharply peaked towards the vertical direction,
of neutrino origin and distributed more nearly isotropically with some slight peaking in the horizontal direction;

pions of low intensity and secondary to the atmospheric muons,
of neutrino origin, being produced in inelastic interactions;

electrons secondary to all muons.

With the present telescopes identification can only be made through the penetrating properties of the particles. Thus, the thickness of lead in telescopes 1 and 2 is sufficient to enable electrons to be distinguished from mesons and the single penetrating particles (as distinct from the 'electron showers' of table 1) are clearly not electrons.

The distinction between pions and muons can only be made in telescopes 3 to 5 with their greater thickness of absorber. So far only one large angle event has been seen in these telescopes; in it, a particle penetrated 3·3 interaction lengths of iron without producing observable secondaries or significant scattering and is identified as a very probable muon. The observation of more such events will enable a firm conclusion to be made about the nature of the neutrino-induced secondaries.

4·2. *Interaction properties of the detected particles*

Of great interest is the problem of the energy of the neutrino secondaries—which will henceforth be referred to as muons. As will be seen later the energy spectrum of detected muons will depend on the details of the production mechanism, being different for intermediate boson decay and inelastic interaction with pion production.

Of subsidiary interest is the energy spectrum of atmospheric muons in so far as its measurement enables a check to be made on the adopted expression for the rate of energy loss of muons at energies to some 4×10^4 to 10^5 GeV.

With the present small number of events a comprehensive analysis cannot be carried out, but already some interesting features are emerging. It can be seen immediately from figure 5 that the degree of accompaniment for particles incident at angles below 40° is significantly greater than that for particles at larger angles. In that figure K denotes a secondary particle (presumably an electron) associated with the penetrating particle (muon), the secondary electron being produced either inside one of the flash-tube trays or in one of the telescope absorbers, or arriving from the rock wall; the number of K's is a rough estimate of the number of electron secondaries. The immediate suggestion is that the mean energy of the atmospheric muons is much greater than that of the muons of neutrino origin.

An attempt has been made to give an estimate of the mean energy in the two cases, although it must be made clear that both the accuracy of the analysis and the statistical precision of the data are, as yet, poor.

The analysis is based mainly on the experimental determination of the frequency of electron secondaries produced in iron and lead absorbers by muons of known energy from the work of Lloyd & Wolfendale (1959) and on the measurements with the Durham horizontal spectograph by Said (1966).

Details of the analysis are given in the appendix; briefly, the conclusion is that the mean energy of the muons with $\phi > 45°$, i.e. muons of mostly neutrino origin, is less than about 30 GeV. The same analysis indicates that the muons with $\phi < 45°$, i.e. mainly of atmospheric origin, have a mean energy of several hundred GeV.

Some information on the lower limit to the muon energies comes from a knowledge of the thickness of absorber in the telescopes penetrated by the particles and their degree of scattering. The former is an instrumental requirement and demands energies greater than 0·1 to 0·2 GeV, depending on obliquity. Of greater significance is the scattering information; no significant scattering has been detected, which indicates that few, if any, of the particles have energy below about 0·7 GeV, a result that is not unexpected since the energy range 0·2 to 0·7 GeV is comparatively narrow. It seems likely, therefore, that the bulk of the muons of neutrino origin lie in the range 0·7 to 30 GeV.

4·3. *Distribution of particles on the celestial sphere*

A study has been made of the arrival directions of all the penetrating particles incident on the telescopes in terms of their celestial coordinates. In telescopes 1 and 2 the projected zenith angle can be measured to about $\pm 1°$ and in telescopes 3 to 5 the spatial angle can be determined to similar accuracy. Muons produced by neutrino interactions are expected to maintain the direction of the initiating particle to within a few degrees. Any grouping of arrival directions on the celestial sphere (over and above that dictated by acceptance criteria) would therefore indicate an extra-terrestial source of some of the neutrinos. K.G.F. is at latitude 12·9° N, longitude 78·3° E and the telescopes are alined with the normals to their detecting faces approximately north–south (telescopes 1 and 2 are 17° W of N and telescopes 3 to 5 are 11° W of N). In a 24 h period the telescopes therefore scan practically the whole of the celestial sphere, although the aperture presented by the telescopes varies considerably with declination (the region from 20° N to the equator has particularly weak coverage).

In presenting the arrival directions we have divided the events into two groups: those plotted in figure 6 for which the projected zenith angle, ϕ, is greater than 45° and those plotted in figure 7, at smaller zenith angles, which will be mainly atmospheric muons. The events may, in general, be produced by upward or downward moving particles and the coordinates of the events are plotted in both hemispheres unless the direction of motion can be deduced from the details of the tracks in the telescopes. The figures give the chronological order of the events: the encircled figures indicate events for which the sense of their motion is known. The uncertainty in azimuth angle of events in telescopes 1 and 2 results in uncertainty in right ascension (and some uncertainty in declination) and the directions of these events thus lie on arcs on the celestial sphere, as shown.

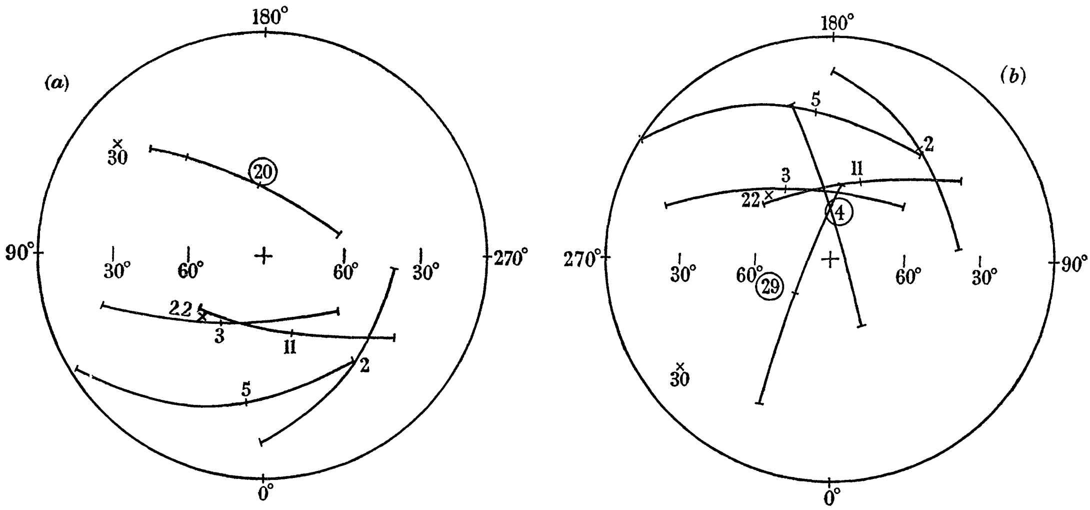

FIGURE 6. Celestial coordinates of detected single particles with projected angle $\phi > 45°$: (*a*) Northern Hemisphere; (*b*) Southern Hemisphere. Ringed numbers indicate particles of known sense of direction. The arcs arise through uncertainty in the azimuthal angles.

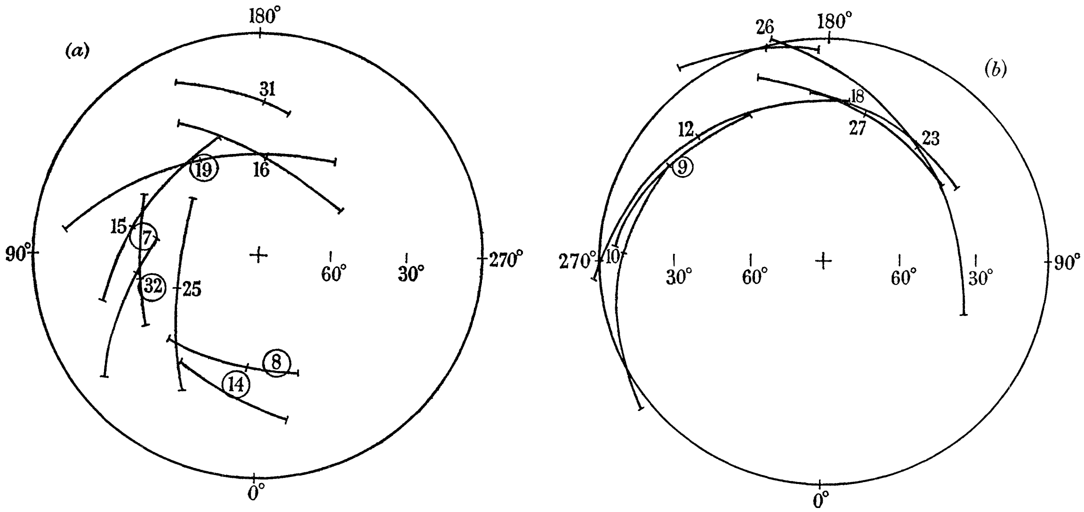

FIGURE 7. Celestial coordinates of detected single particles with $\phi < 45°$: (*a*) Northern Hemisphere; (*b*) Southern Hemisphere. The grouping in *declination* arises from the sharply peaked angular distribution of the atmospheric muons taken together with the geometrical acceptance of the telescopes.

A breakdown of the total running time achieved to date into hourly periods of sidereal time shows that the scan has been uniform in sidereal time to within $\pm 10\%$. This implies that for an isotropic flux of primary particles the distribution of events should be symmetrical in Right Ascension. As can be seen from figure 6 the neutrino events as yet show no obvious asymmetry; this is of course hardly surprising in view of the small number of particles so far detected and the uncertainties of location.

In figure 7 the atmospheric muon events are shown. Muons penetrating to a depth of 7500 m.w.e. with zenith angle 35° have an average energy at sea level of about 10^4 GeV and would come from parent primaries of energy 10^5 to 10^6 GeV. There is some slight evidence for asymmetry in these events, there being a gap between 21 and 4 h in the Southern Hemisphere and between 17 and 22 h in the Northern Hemisphere but the statistical accuracy is as yet too poor for certainty.

4·4. *Comparison of the observed rate with prediction*

4·4·1. *The energy spectrum of neutrinos underground*

The expected numbers of neutrino-induced muons have been calculated for a variety of assumed neutrino cross-sections using the derived neutrino energy spectra. The latter come from an analysis of the propagation of cosmic rays in the

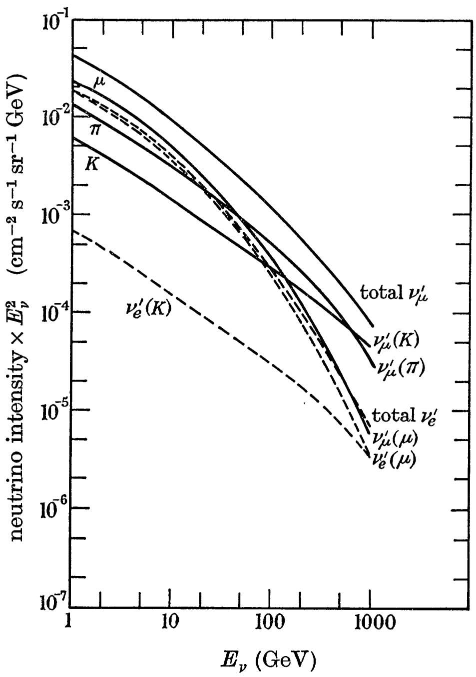

FIGURE 8. Energy spectrum of atmospheric neutrinos in the horizontal direction. (ν' signifies $\nu+\bar{\nu}$.) The parent particles are indicated.

atmosphere and have been reported, with increasing accuracy, by Greisen (1960), Zatsepin & Kuzmin (1962), Cowsik *et al.* (1963, 1966) and Osborne, Said & Wolfendale (1965). The energy spectrum in the horizontal direction calculated by Osborne *et al.* is shown in figure 8. It is seen that up to about 50 GeV the bulk of the muon neutrinos come from $\mu-e$ decay, the large contribution arising from the enhanced probability of $\mu-e$ decay in the long path encountered between the production levels and ground level.

4·4·2. *Neutrino interaction processes*

The contributions to the underground muon flux from the following processes have been considered:

(i) Elastic collisions,
$$\nu_\mu + N \rightarrow \mu + N'; \tag{1}$$
(ii) Inelastic collisions,
$$\nu_\mu + N \rightarrow \mu + N' + \pi\text{'s}, \quad \text{etc.}; \tag{2}$$
(iii) Production of intermediate boson W,
$$\nu_\mu + N \rightarrow N + \mu + W \text{ (incoherent production)}, \tag{3}$$
$$\nu_\mu + Z \rightarrow Z + \mu + W \text{ (coherent production)}, \tag{4}$$
$$\bar{\nu}_e + e^- \rightarrow W^- \text{ (Glashow resonance)}. \tag{5}$$

In each of the reactions (3), (4) and (5) it is assumed that some of the W's decay by a leptonic mode
$$W \rightarrow \mu + \nu_\mu.$$

Below 10 GeV neutrino energy the cross-sections adopted for the comparison are taken from the direct observations at C.E.R.N. and at higher energies alternative assumptions are made about the form of the cross-sections. The details are summarized in table 3. The calculations given in earlier publications were based mainly on the work of Block *et al.* 1964; more recent measurements and analyses (E.C.M. Young, private communication, 1966) have indicated somewhat

TABLE 3. NEUTRINO CROSS-SECTIONS AND EXPECTED NUMBERS OF EVENTS

interaction	cross-section	fraction of energy taken by muon	no. of events	approx. median neutrino energy (GeV)
(1) elastic	0.6×10^{-38} per $n-p$ pair	0·9	0·7	2·5
	(0.75×10^{-38})	(1·0)	(1·0)	
(2) inelastic				
$E_\nu < 10$ GeV	$0.30E_\nu \times 10^{-38}$ cm² per nucleon	0·67	1·1	—
	$(0.45E_\nu \times 10^{-38})$	(0·50)	(1·3)	
$E_\nu > 10$ GeV	case (*a*) $0.30E_\nu \times 10^{-38}$ for all E_ν	0·67	2·7	25
	$(0.45E_\nu \times 10^{-38})$	(0·50)	(3·0)	
	case (*b*) 3.0×10^{-38}	1·0	0·9	9
	(4.5×10^{-38})	(1·0)	(1·3)	
(3), (4) boson production	$M_W = 1.8$ GeV	near threshold	4·2	100
		[asymptotic]	[15]	
	$M_W = 2.5$ GeV	near threshold	1·9	200
		[asymptotic]	[6·9]	
(5) Glashow resonance	$M_W = 1.8$ GeV	0·25	1·3	3000
	$M_W = 2.5$ GeV	0·25	0·3	6000
	upper limit: $M_W = 1.8$ GeV and case (*a*)		10	
	lower limit: $M_W \gg 1.8$ GeV and case (*b*)		2·7	

The numbers in round brackets refer to our earlier assumptions (Achar *et al.* 1965*c*).

different values and these have been adopted in the present work. The earlier assumptions and their resulting predicted numbers are given in round brackets.

The cross-sections for processes (3), (4) and (5) depend on the mass of the intermediate boson M_W. It is known from the C.E.R.N. and Brookhaven neutrino experiments (Bernardini *et al.* 1964; Burns *et al.* 1965) that $M_W > 1{\cdot}8$ GeV. The production cross-sections for incoherent and coherent interactions have been taken from the calculations of Wu *et al.* (as quoted by Burns *et al.* 1965) up to $E_\nu = 20$ GeV and those of von Gehlen (1963) which give the asymptotic limit, valid above 100 GeV. An interpolation has been made for the region 20 to 100 GeV. At energies near threshold the incoherent process dominates the coherent interaction and at higher energies ($E_\nu \geqslant 50$ GeV) the situation is reversed.

The contribution from process (5) has been calculated from the work of Zagrebin & Zheleznykh (1964). This contribution is small compared with (3) and (4) mainly because at the resonance energies ($E_\nu \simeq 1000\, M_W^2$ GeV, for M_W in GeV) the flux of anti-electron neutrinos is very small.

In addition to taking the relevant cross-sections it is necessary to adopt a value for the fraction of the incident neutrino energy carried by the muon (or muons) after the interaction. The values used for the elastic and inelastic processes are given in table 3. There is uncertainty in the boson case and this reflects as uncertainty in the predicted rates. For boson production by comparatively low energy neutrinos the momentum transfer to the nucleon is large and the energy spectrum of prompt muons is strongly affected by the form factor of the nucleon. The spectrum is peaked at $E_\nu M_\mu/(M_W+M_\mu)$ corresponding to the minimum momentum transfer $M_W^2/2E_\nu$. This situation applies for $M_W = 1{\cdot}8$ GeV and $E_\nu \sim 10$ GeV. For very high energies the asymptotic formula given by Lee, Markstein & Yang (1961) gives $\bar{E}_\mu \simeq \frac{1}{2}E_\nu$. Von Gehlen (1963) indicates that the interaction cross-sections correspond to the asymptotic formula of Lee *et al.* only at energies greater than 10^4 GeV.

The branching ratio expected for the muon decay mode of the W is not known but we have calculated for an assumed ratio of 40 %. Uberall (1964) has suggested that the W is strongly polarized and comes out predominantly backwards in the C-system. The delayed muon then retains about one quarter of the boson energy. The two limiting conditions are thus:

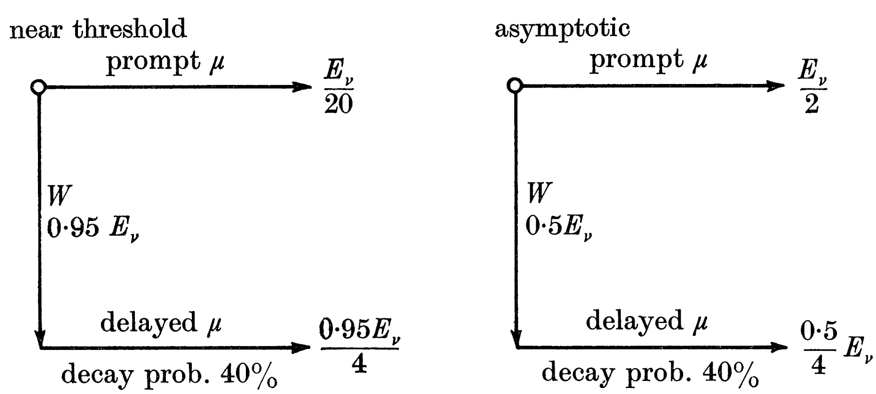

In that the neutrino energies contributing most are near threshold the asymptotic values must be regarded as extreme upper limits; they are indicated in the table but not used in the analysis.

4·4·3. *Calculation of the predicted rates*

The cross-sections discussed above have been used, together with the neutrino spectra as a function of zenith angle, the range-energy relation for muons and the geometrical acceptance of the telescopes, to calculate the predicted rates of events. The numbers expected in the sensitive time of 16, 915 m^2 day sterad are indicated

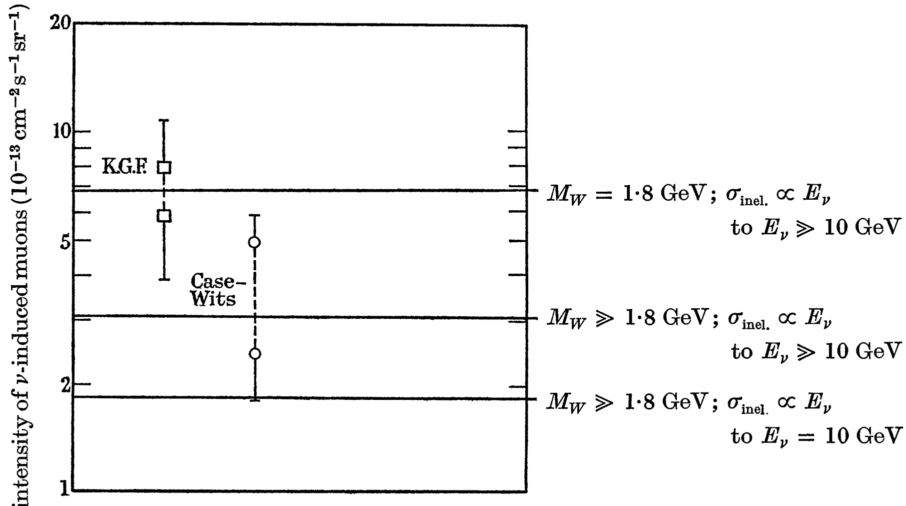

FIGURE 9. Comparison of the detected rate of ν-events with expectation and with the results of the Case–Wits experiment. In the K.G.F. results the upper point corresponds to 11 events and the lower to 8 events (see p. 144). The two Case–Wits points refer to calculations made by us with inclusion, and exclusion, of their multi-tank events.

in table 3. Taking the 'Near threshold' condition and M_W = 1·8 GeV together with case (*a*) for the inelastic cross-section the upper limit to the number of events expected is 10. Similarly, the lower limit is 2·7 events, for case (*b*) and $M_W \gg$ 1·8 GeV. The observed number (8 to 11) is between these limits. The data are plotted in the form of muon intensities in figure 9, where the same comparison can be made.

Figure 9 also shows the rate determined by the Case–Wits group (Crouch *et al.* 1966); it is apparent that there is no inconsistency between the two measurements. It is also clear that, in agreement with the accelerator results the boson mass certainly cannot be much less than 1·8 GeV.

From observations of rate alone it cannot be established that the boson exists; even with excellent statistical accuracy there would be no possibility of distinguishing between contributions from bosons and from inelastic interactions. Other possible ways of settling the problem are discussed later.

4·5. *The energy spectrum of the detected muons*

The neutrino cross-sections described above (see table 3—non-bracketed values) have been taken together with the neutrino energy spectrum to give the energy spectra expected for the muons at large zenith angles. The calculation of the high energy end of the spectrum is subject to uncertainty in that it requires extrapolations of the neutrino intensity and the cross-sections to very high energy and the calculated mean energies are therefore also uncertain.

The mean energy for the case of a cross-section increasing linearly with E_ν *ad infinitum* is about 160 GeV and the median energy is about 13 GeV. These values drop considerably if the increase in cross-section is terminated; thus, using the data of Cowsik *et al.* (1966) the median energies are found to be *ca.* 8 GeV for a cut-off at 100 GeV and *ca.* 3 GeV for a cut-off at 20 GeV.

If the intermediate boson exists, with $M_W = 1{\cdot}8$ GeV, the mean muon energy is about 37 GeV and the median is *ca.* 10 GeV.

The mean values of R expected for both inelastic (with no cut-off) and boson interactions are shown in figure 13. (See appendix for discussion of the significance of R.) Clearly, the statistical accuracy attained so far is insufficient to decide between the two possibilities, but two facts emerge:

(*a*) if, with improved statistics, the rate should be lower than our present value showing that either the W-mass is greater or the inelastic cross-section is cut off then the predicted mean energy for W-production will increase and for inelastic production $\bar{E}_\mu$ will fall. A distinction should then be possible.

(*b*) the muon momenta are probably low enough to allow magnetic deflexion techniques to work and thus enable direct measurements to be made.

4·6. *Multiple events*

Two events have been recorded in which a penetrating particle incident at a large angle has been observed in association with other particles. In neither case is the accompaniment electromagnetic in character. The events are shown in figures 17 and 18, plates 22 and 23.

Event no. 4 has been discussed in detail by Achar *et al.* 1965*b*; briefly, it is considered that it represents the interaction products of an upward moving neutrino which interacts non-elastically in the rock near the apparatus.

Event no. 29 is not as clear cut but the most likely explanation is that this too represents a non-elastic interaction, as indicated in figure 18.

The question of great contemporary interest is whether or not these interactions were mediated by the intermediate boson. A clear answer is not possible in view of the lack of precise knowledge of the nature of the detected particles. Thus, the tracks in events 4 and 29 could be due to pions or muons (or a mixture).

5. Conclusions and future plans

5·1. *Conclusions at the present stage*

Since the number of events detected is still small the conclusions to be drawn are in general only tentative. It is, however, clear that there is firm visual evidence for the existence of the secondaries of neutrino interactions, the secondaries being, in the main, very probably muons of energy below about 30 GeV. In two cases there is evidence that the secondaries are upward moving—a sure indication of neutrino origin.

The number of events detected is roughly a factor of two greater than that expected from an extrapolation of the accelerator cross-sections to higher energies. If this result is not due to an upward statistical fluctuation it suggests that either the inelastic cross-section increases more rapidly than has been assumed above 10 GeV or that the intermediate boson exists with a mass not much above 1·8 GeV.

To turn to the celestial coordinates of the detected neutrino-induced particles, there is no indication, as yet, for any interesting grouping on the celestial sphere, but this is hardly surprising in view of the small numbers and uncertainties of location.

5·2. *Future plans*

It is clear that increased numbers of events are essential and it is intended to continue to operate the five telescopes.

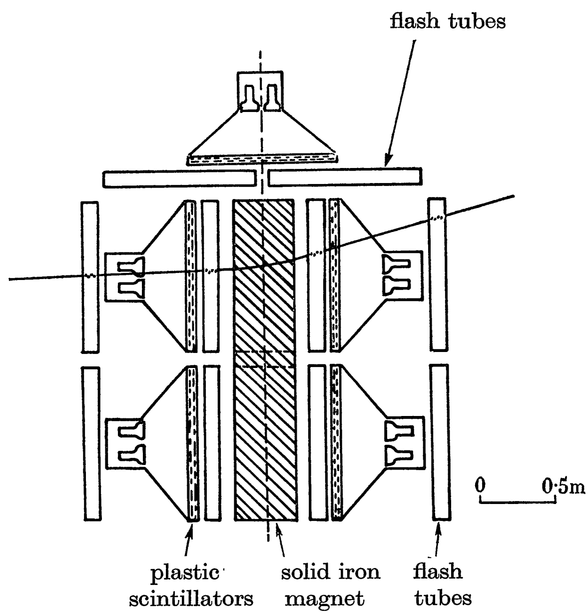

Figure 10. Magnetic spectrograph under construction.

A promising method of detecting the intermediate boson is to search for double muons which have their point of origin deep in the rock; telescopes 3 to 5 are designed for this purpose. If the boson does exist, with mass below about 4 GeV, it should be detectable this way.

As a further aid to distinguishing intermediate boson products from those of inelastic interactions, momentum and sign resolution will be possible with magnetic spectrographs. Two such instruments of the design shown in figure 10 are at present under construction; each will have a collecting power of about 25 m^2 sr and a maximum detectable momentum of about 20 GeV/c.

Appendix. Estimation of the mean energy of the underground muons

The principle of the method can be seen from figure 11 which shows the frequency of electron events produced in iron by muons in the momentum range 5 to 1000 GeV/c (Said 1966). The rapid rise in the frequency of electron showers, which is such a prominent feature of the observations, is caused mainly by the increased contribution from direct electron pair production. It is clear that with sufficient numbers of traversals of local absorbers and the observation of the secondary electrons produced, an estimate of the mean energies in the underground experiment should be possible.

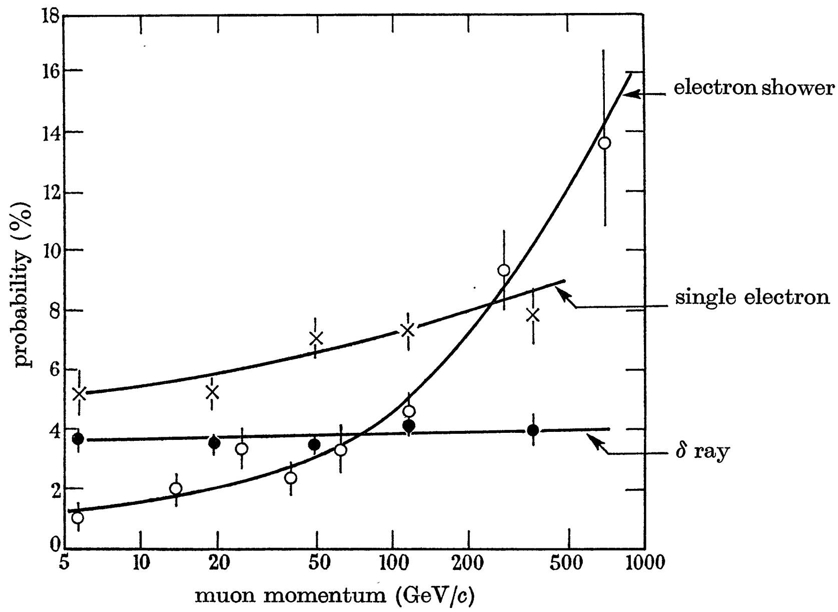

Figure 11. Electromagnetic interactions of muons in iron (Said 1966). The curves are lines drawn through the experimental points.

The limited experimental data on accompaniment have been combined in the following way. The electron secondaries seen on the flash-tube photographs have been allocated to the categories shown in figure 11, namely δ-rays (i.e. electrons produced within the flash-tube trays) single electrons, coming from outside the trays and electron showers, also coming from outside. From the observations of a number of other experiments statistical weights have been applied to the categories to give the equivalent number of electron tracks crossing a flash-tube tray and a quantity R has been derived for each event given by

$$R = 1 + 0{\cdot}7f_1 + f_2 + 3f_3.$$

Here, f_1, f_2 and f_3 are the observed probabilities per tray of the occurrence of δ-rays, single electrons and showers and are thus 0, $\frac{1}{3}$, $\frac{2}{3}$ or 1, and the first term represents the incident muon itself. For example, an event in which a muon passed through three trays and was accompanied by a single knock-on electron in one of them would give $R = 1{\cdot}33$.

The R values for the individual events are shown in figure 12 plotted against the projected zenith angle. The out-of-geometry muons are used in so far as production of secondaries inside the telescopes is taken into account, but the electrons accompanying the muon, which provided at least part of the trigger, are not included in the determination of R.

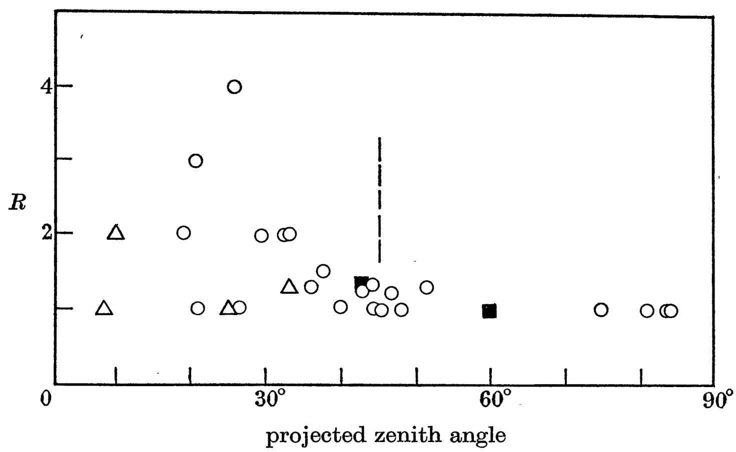

FIGURE 12. Accompaniment of K.G.F. events. ○, Telescopes 1 and 2, in geometry; ■, telescopes 3 to 5, in geometry; △, out of geometry.

The expected mean values of R as a function of muon energy have been calculated from the work already indicated, corrections and conversions being applied wherever necessary to make the results applicable in the present case of lead-, iron- and rock-producing layers.

The results of Creed *et al.* (1965) in which the electromagnetic interactions of

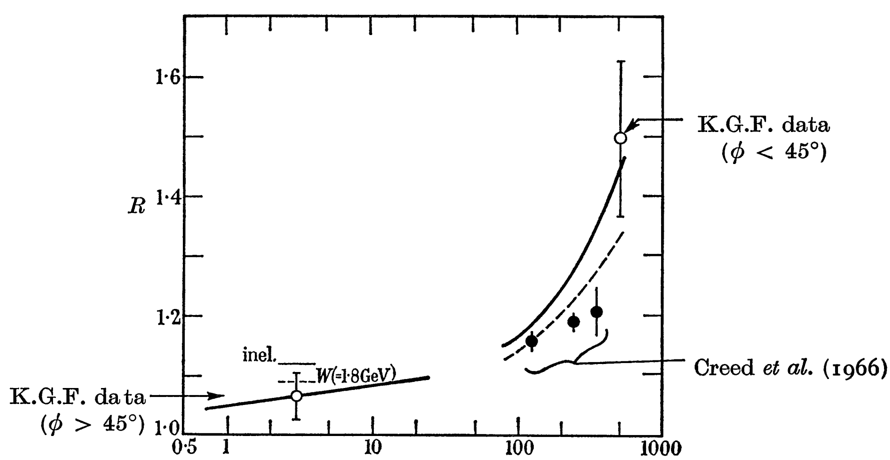

FIGURE 13. Variation of R with muon energy. The 'Creed *et al.* data' are to be compared with the dotted curve and the 'K.G.F. data' with the full line. (See 'Note added in proof', after References.)

muons underground were studied down to great depths have been used to give the effect of muon trajectory obliquity on shower production probability. The expected variation is shown in figure 13. Also shown are the mean values of R for the present work, divided according to $\phi > 45°$ and $\phi < 45°$, i.e. (mainly) neutrino muons and atmospheric muons.

Using the value of R for $\phi > 45°$ the effective mean energy of the neutrino-induced muons is seen to be below about 30 GeV and the point is plotted at the best estimate of 3 GeV.

The value of R for $\phi < 45°$ is plotted at an energy of 460 GeV, this being the approximate mean energy at 7500 m.w.e. for muons incident at a mean zenith angle of 35° calculated by means of the treatment given by Mikhalchi & Zatsepin (1965). (But see 'Note added in proof' after References.)

In addition to the present data the results of Creed *et al.* (1965) (on atmospheric muon interactions at shallower depths) have been treated in the same way and the mean values of R have been plotted at the appropriate expected mean energies. The near agreement with expectation for all the atmospheric muon data suggests that the adopted method is not too inaccurate.

The authors wish to thank Dr P. K. MacKeown, Dr P. V. Ramana Murthy, Mr A. M. Vinze and Mr R. M. Wankar for their efforts on the experiment and Dr E. C. M. Young for useful discussions.

The Science Research Council (U.K.) and the Japanese Association for the promotion of Science are thanked for their support and we are grateful to Mr M. Yukawa of the Yawata Iron Works for donating the iron for the magnetic spectrographs.

We are grateful to the Kolar Gold Mine Undertaking authorities and the staff for their ready cooperation, in particular to Mr M. H. Parthasarathy, the Managing Director, Mr V. V. R. Rao, the former Superintendent Mr P. Vijayaraghavan, the present Superintendent and Mr A. Seetharam, Chief Mechanical Engineer of Champion/Mysore Mines.

References (Menon *et al.*)

Achar, C. V., Menon, M. G. K., Narasimham, V. S., Ramana Murthy, P. V., Sreekantan, B. V., Hinotani, K., Miyake, S., Creed, D. R., Osborne, J. L., Pattison, J. B. M. & Wolfendale, A. W. 1965*a* *Phys. Lett.* **18**, 196; 1965*b* *Phys. Lett.* **19**, 78; 1965*c* *Proc. Int. Conf. on Cosmic Rays, London*, p. 1012.

Bernardini, G., Bienlein, J. K., von Dardel, G., Faissner, H., Ferrero, F., Gaillard, J. M., Gerber, H. J., Hahn, B., Kaftanov, V., Krienen, F., Manfredotti, C., Reinharz, M. & Salmeron, R. A. 1964 *Phys. Lett.* **13**, 86.

Block, M. M., Burmeister, H., Cundy, D. C., Eiben, B., Franzinetti, C., Keren, J., Møllerud, R., Myatt, G., Orkin-Lecourtois, A., Paty, M., Perkins, D., Ramm, C. A., Schultze, K., Sletten, H., Soop, K., Stump, R., Venus, W. & Yoshiki, H. 1964 *Phys. Lett.* **12**, 281.

Burns, R., Goulianos, K., Hyman, E., Lederman, L., Lee, W., Mistry, N., Rettberg, J., Schwartz, M., Sunderland, J. & Danby, G. 1965 *Phys. Rev. Lett.* **15**, 42.

Cowsik, R., Pal, Y., Rengarajan, T. N. & Tandon, S. N. 1963 *Proc. Int. Conf. on Cosmic Rays, Jaipur* **6**, 211.

Cowsik, R., Pal, Y. & Tandon, S. N. 1966 *Proc. Ind. Acad. Sci.* **53**, 217.

Creed, D. R., Pattison, J. B. M., Wolfendale, A. W., Achar, C. V., Narasimham, V. S. & Ramana Murthy, P. V. 1965 *Proc. Int. Conf. on Cosmic Rays, London*, p. 980.

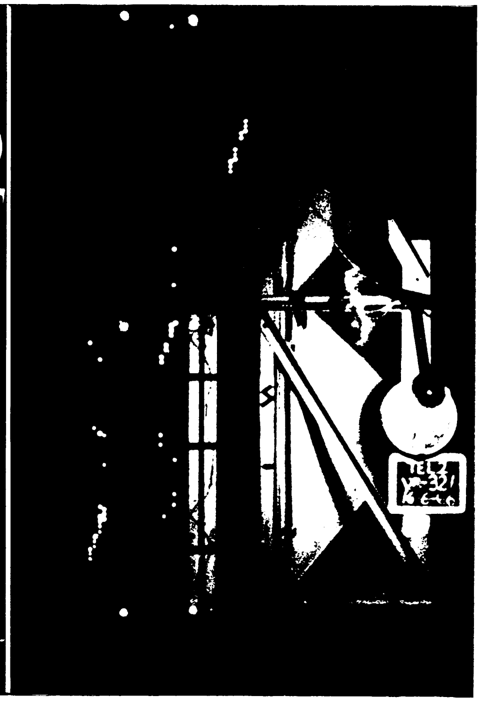

FIGURE 14

FIGURE 15

FIGURE 14. Atmospheric muon producing a dense electromagnetic shower in the lead absorber (event no. 9). Note: the three pairs of uniformly spaced white dots (top, centre and bottom) on this, and all the Plates, are the images of fiducial bulbs.

FIGURE 15. Atmospheric muon producing weak electromagnetic shower in the lead absorber (event no. 26).

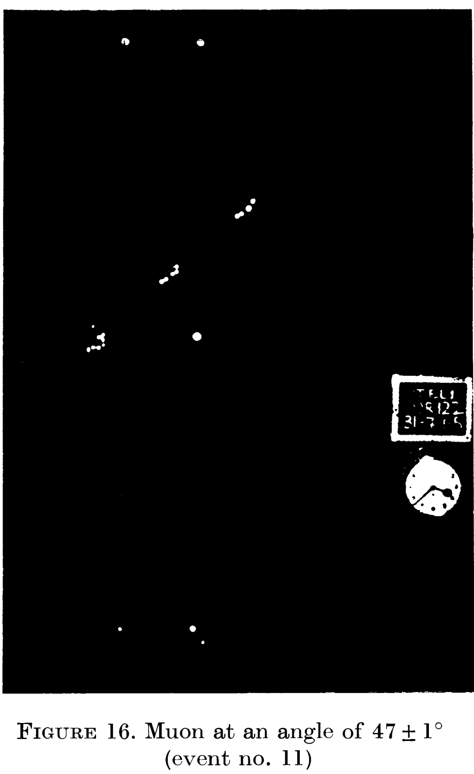

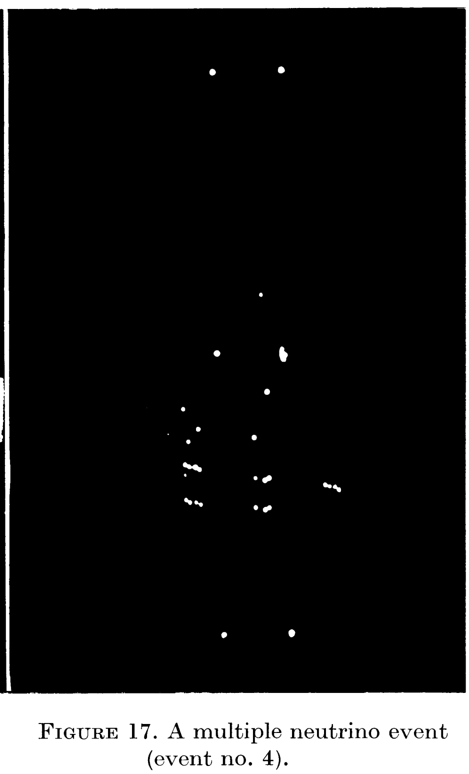

FIGURE 16. Muon at an angle of $47 \pm 1^\circ$ (event no. 11)

FIGURE 17. A multiple neutrino event (event no. 4).

(*Facing p.* 156)

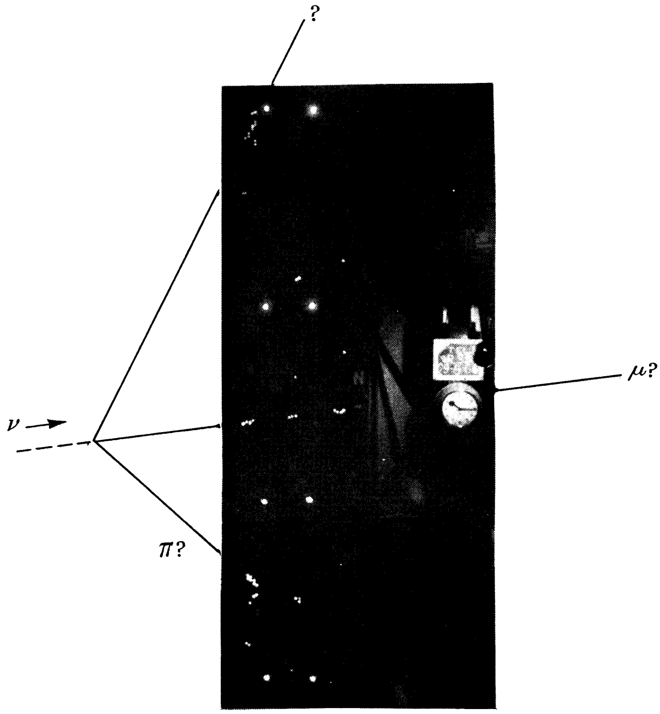

FIGURE 18. A multiple neutrino event (event no. 29).

FIGURE 19. A small electron shower (event no. 21).

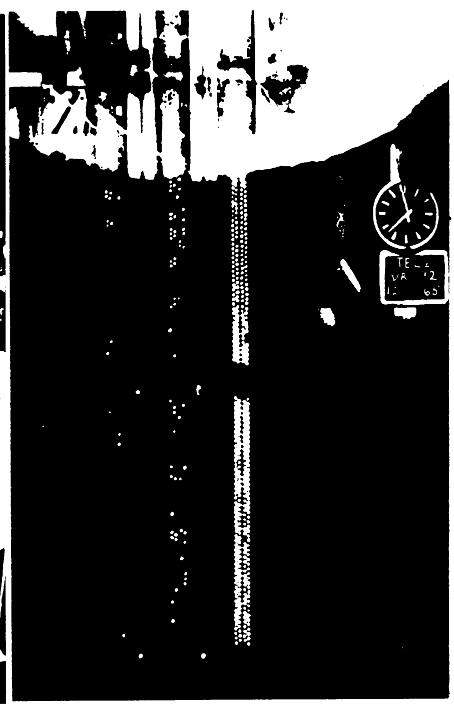

FIGURE 20. A dense electron shower (event no. 13).

Crouch, M. F., Kropp, W. R., Gurr, H. S., Sobel, H., Meyer, B., Sellschop, J. P. F. & Reines, F. 1966 *Proc. Rochester Conference, Berkeley* (in the Press).
Greisen, K. 1960 *Proc. Int. Conf. for Instrumentation in High Energy Physics, Berkeley*, p. 209. New York: Interscience.
Lee, T. D., Markstein, P. & Yang, C. N. 1961 *Phys. Rev. Lett.* **7**, 429.
Lloyd, J. L. & Wolfendale, A. W. 1959 *Proc. Phys. Soc.* **73**, 178.
Menon, M. G. K., Naranan, S., Narasimham, V. S., Hinotani, K., Ito, N., Miyake, S., Creed, D. R. Osborne, J. L., Pattison, J. B. M. & Wolfendale, A. W. 1967 *Proc. Phys. Soc.* **90**, 649.
Mikhalchi, E. D. & Zatsepin, G. T. 1965 *Proc. Int. Conf. on Cosmic Rays, London*, p. 997.
Osborne, J. L., Said, S. S. & Wolfendale, A. W. 1965 *Proc. Phys. Soc.* **86**, 93.
Reines, F., Crouch, M. F., Jenkins, T. L., Kropp, W. R., Gurr, H. S., Smith, G. R., Sellschop, J. P. F. & Meyer, B. 1965 *Phys. Rev. Lett.* **15**, 429.
Said, S. S. 1966 Ph.D. thesis, University of Durham.
Uberall, H. 1964 *Phys. Rev.* **133**, B 444.
von Gehlen, G. 1963 *Nuovo Cim.* **30**, 859.
Zagrebin, V. A. & Zheleznykh, I. M. 1964 Preprint Lebedev Institute, Moscow.
Zatsepin, G. T. & Kuzmin, V. A. 1962 *Soviet Phys. JEPT* **14**, 1294.

Note added in proof

The Mikhalchi & Zatsepin treatment was applied incorrectly and the quoted mean energy of 460 GeV is in error; it should be rather less than 300 GeV. However, a more recent reappraisal of the angular distribution of atmospheric muons suggests that the adopted form of the depth-intensity curve may be inaccurate; if a more slowly varying form is used the mean energy will approach the value shown in the figure.

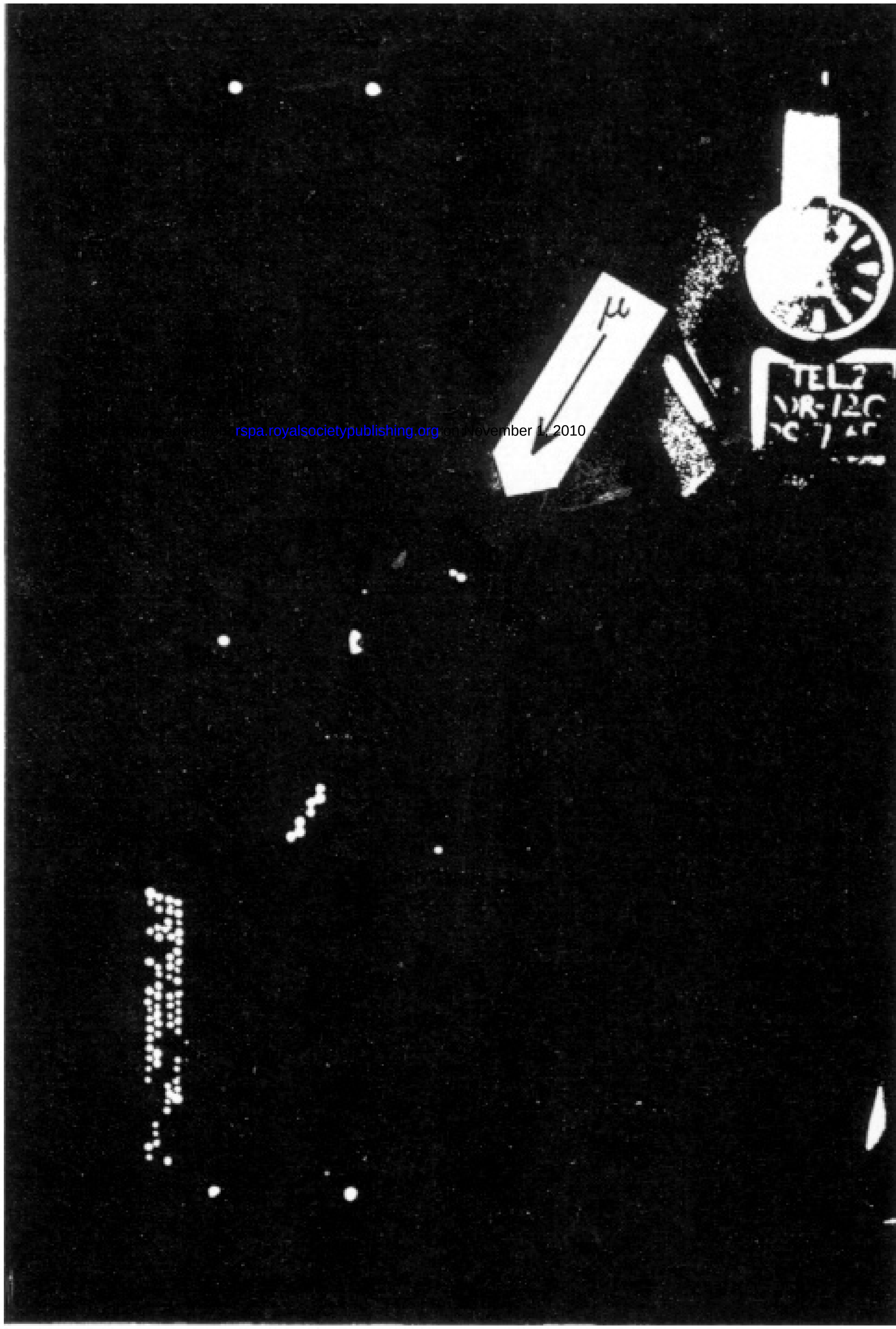

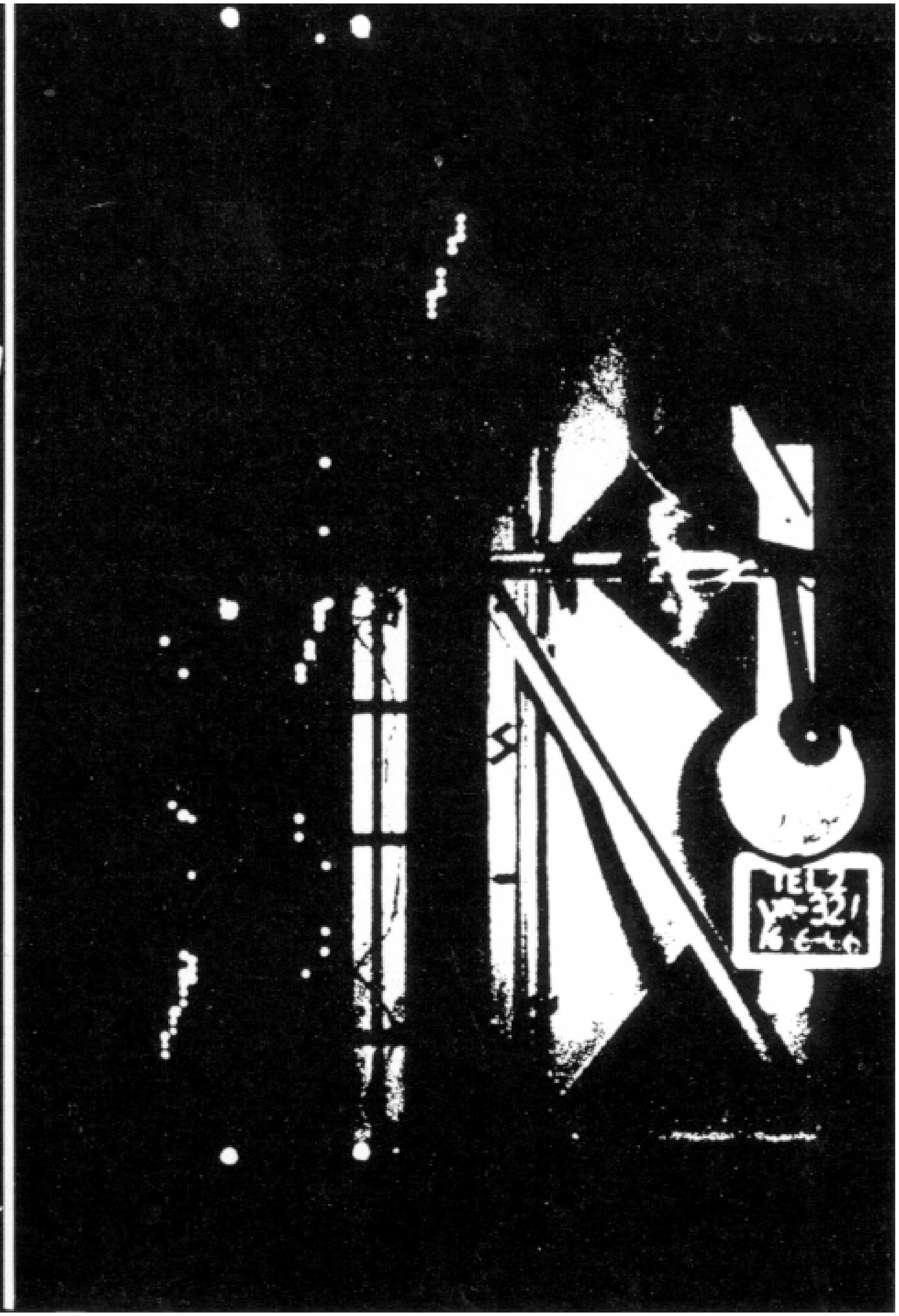

FIGURE 14

FIGURE 15

FIGURE 14. Atmospheric muon producing a dense electromagnetic shower in the lead absorber (event no. 9). Note: the three pairs of uniformly spaced white dots (top, centre and bottom) on this, and all the Plates, are the images of fiducial bulbs.

FIGURE 15. Atmospheric muon producing weak electromagnetic shower in the lead absorber (event no. 26).

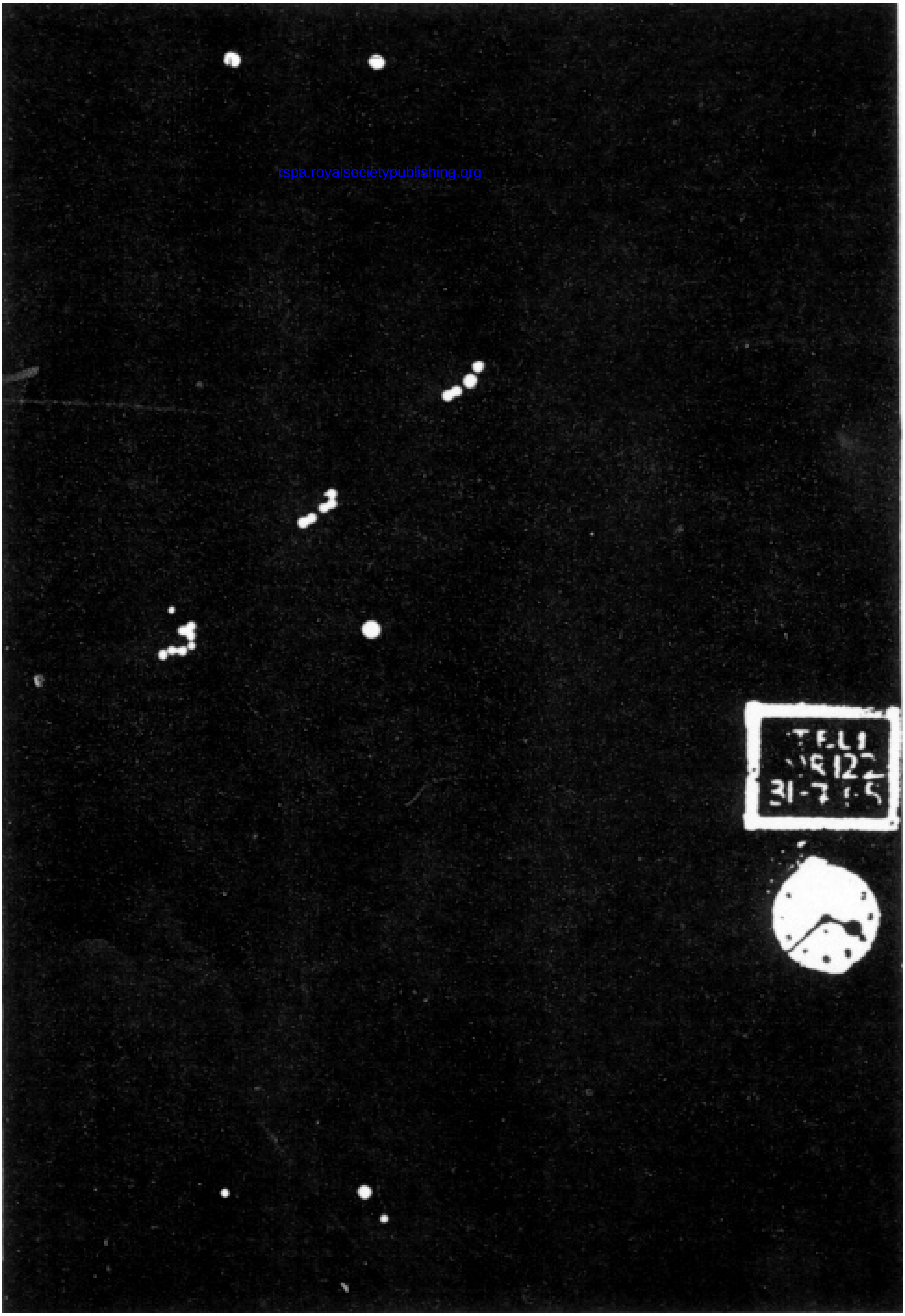

FIGURE 16. Muon at an angle of $47 \pm 1^{\circ}$ (event no. 11)

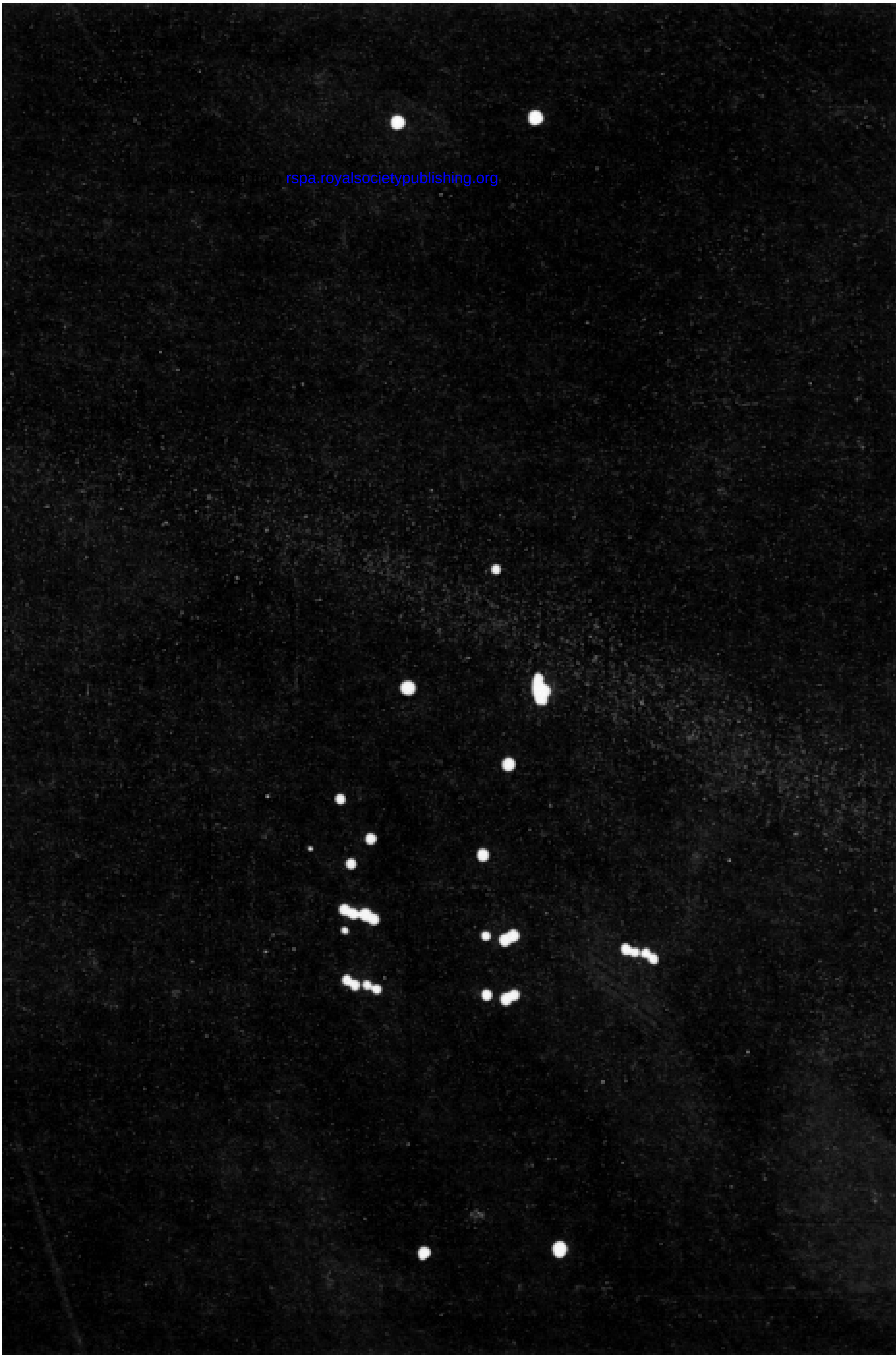

FIGURE 17. A multiple neutrino event (event no. 4).

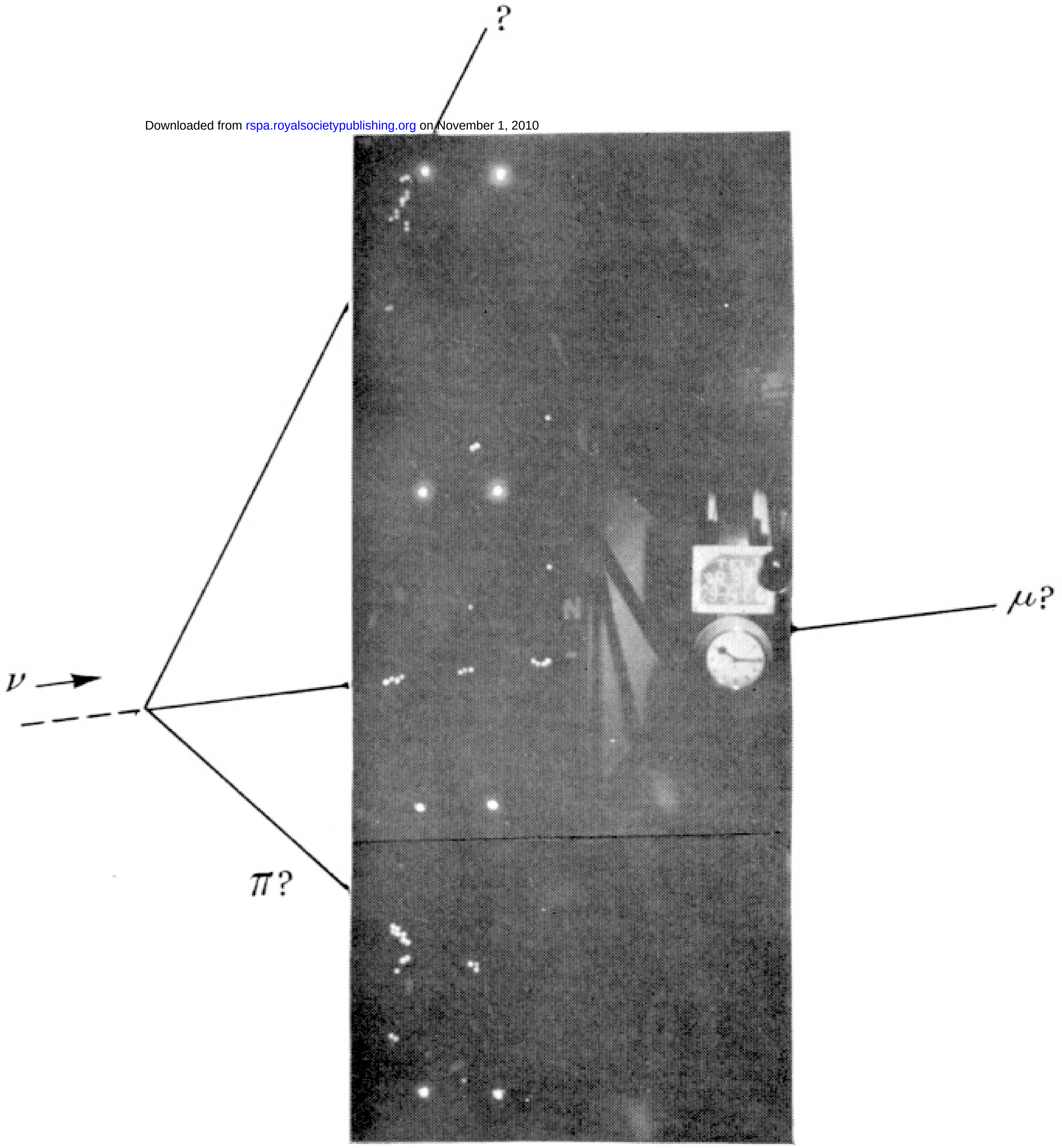

FIGURE 18. A multiple neutrino event (event no. 29).

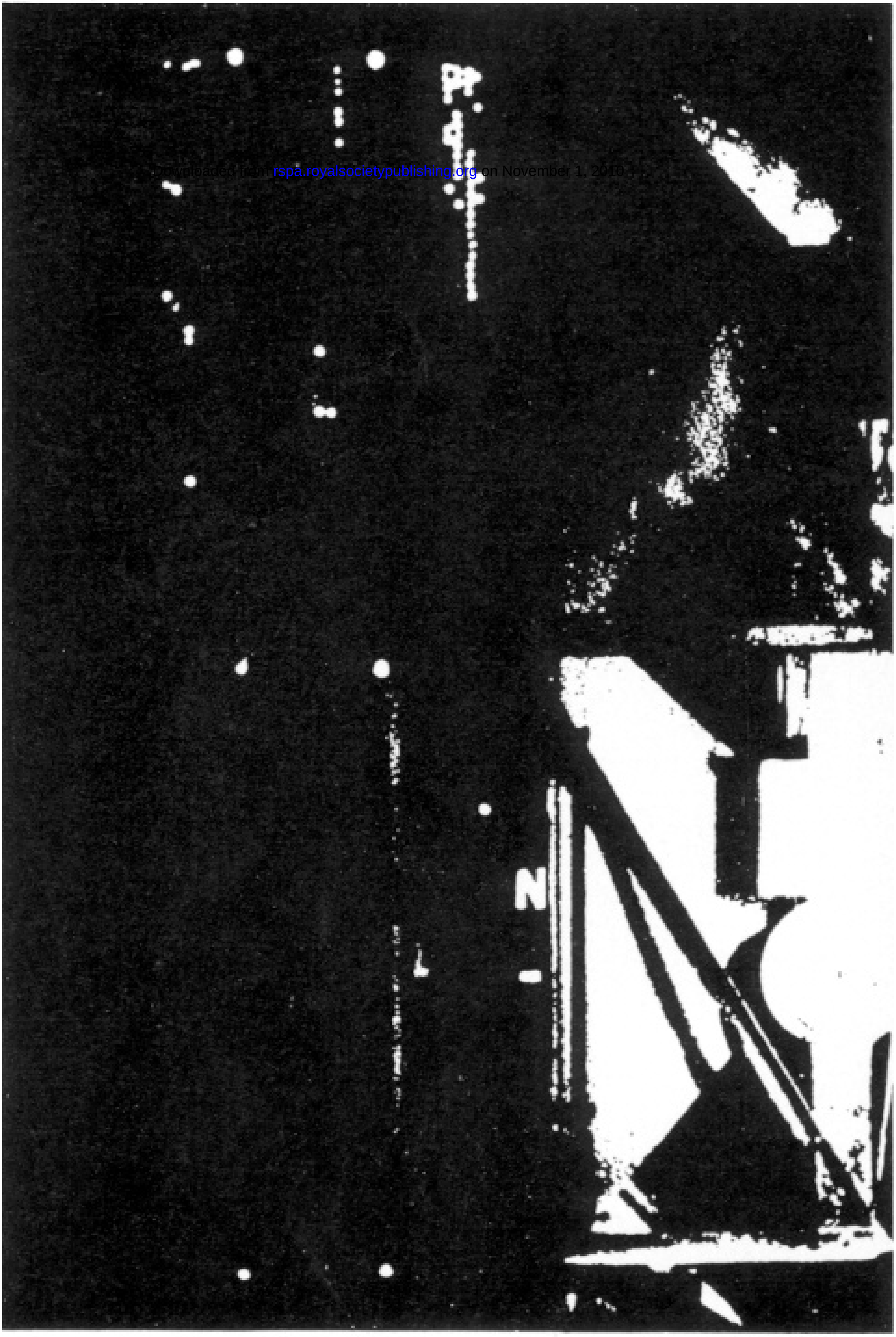

FIGURE 19. A small electron shower (event no. 21).

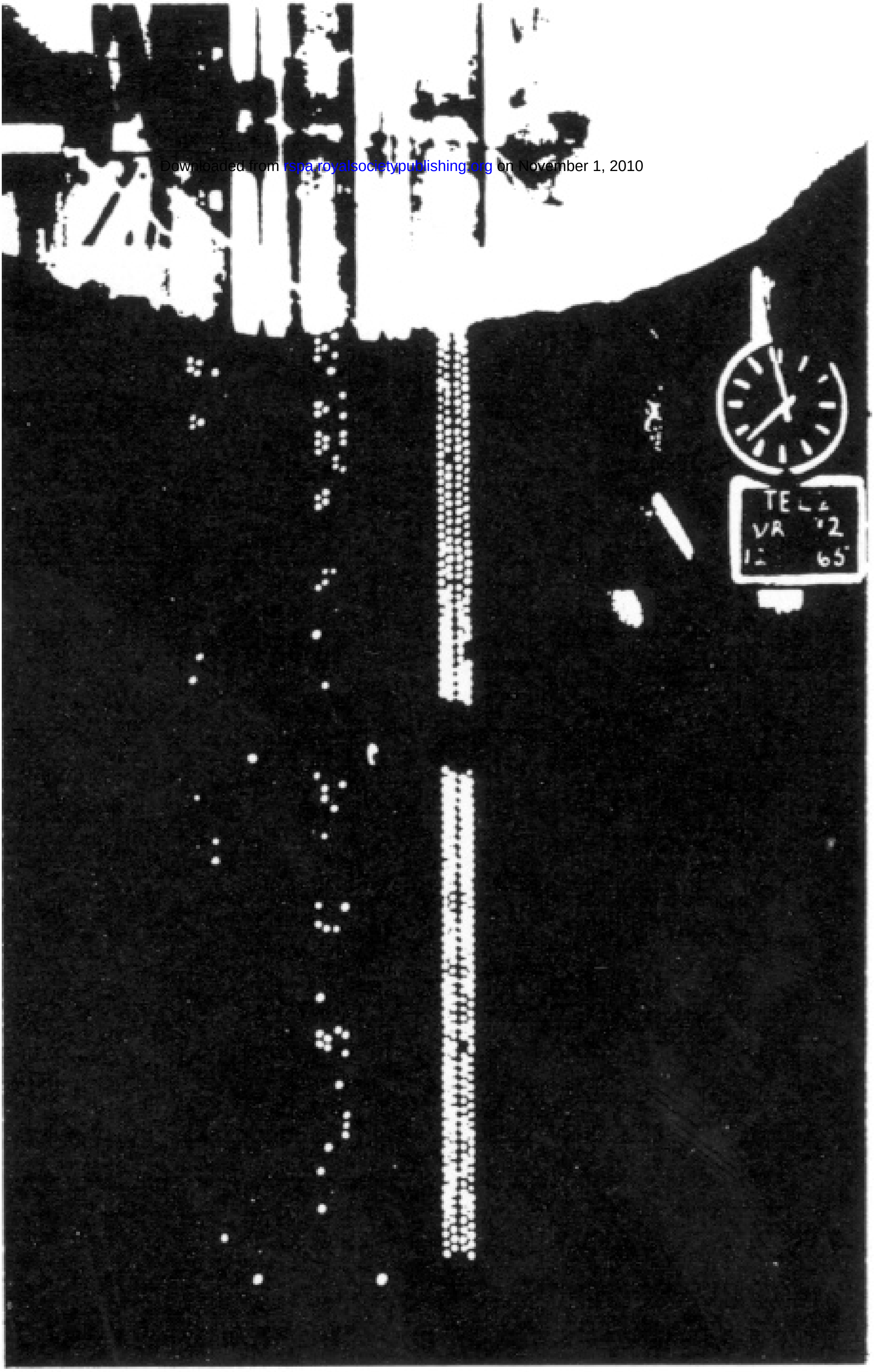

FIGURE 20. A dense electron shower (event no. 13).